AMERICAN SOCIETY FOR MICROBIOLOGY | mSphere®

RESEARCH ARTICLE
Molecular Biology and Physiology

Pyrophosphate Stimulates the Phosphate-Sodium Symporter of *Trypanosoma brucei* Acidocalcisomes and *Saccharomyces cerevisiae* Vacuoles

Evgeniy Potapenko,[a,b] Ciro D. Cordeiro,[a,b] Guozhong Huang,[a,b] Roberto Docampo[a,b]

[a]Center for Tropical and Emerging Global Diseases, University of Georgia, Athens, Georgia, USA
[b]Department of Cellular Biology, University of Georgia, Athens, Georgia, USA

ABSTRACT Inorganic pyrophosphate (PP_i) is a by-product of biosynthetic reactions and has bioenergetic and regulatory roles in a variety of cells. Here we show that PP_i and other pyrophosphate-containing compounds, including polyphosphate (polyP), can stimulate sodium-dependent depolarization of the membrane potential and P_i conductance in *Xenopus* oocytes expressing a *Saccharomyces cerevisiae* or *Trypanosoma brucei* Na^+/P_i symporter. PP_i is not taken up by *Xenopus* oocytes, and deletion of the TbPho91 SPX domain abolished its depolarizing effect. PP_i generated outward currents in Na^+/P_i-loaded giant vacuoles prepared from wild-type or *pho91*Δ yeast strains expressing *TbPHO91* but not from the *pho91*Δ strains. Our results suggest that PP_i, at physiological concentrations, can function as a signaling molecule releasing P_i from *S. cerevisiae* vacuoles and *T. brucei* acidocalcisomes.

IMPORTANCE Acidocalcisomes, first described in trypanosomes and known to be present in a variety of cells, have similarities with *S. cerevisiae* vacuoles in their structure and composition. Both organelles share a Na^+/P_i symporter involved in P_i release to the cytosol, where it is needed for biosynthetic reactions. Here we show that PP_i, at physiological cytosolic concentrations, stimulates the symporter expressed in either *Xenopus* oocytes or yeast vacuoles via its SPX domain, revealing a signaling role of this molecule.

KEYWORDS SPX domain, *Saccharomyces cerevisiae*, *Trypanosoma brucei*, *Xenopus laevis*, acidocalcisome, phosphate-sodium symporter, pyrophosphate

Inorganic pyrophosphate (PP_i) is a side product of more than 200 biosynthetic reactions, like the synthesis of isoprenoids, nucleic acids, proteins, and coenzymes and the activation of fatty acids (1). Hydrolysis of PP_i by pyrophosphatases (PPases) has been recognized to make these biosynthetic reactions thermodynamically favorable (2). PP_i also has bioenergetic functions and regulatory roles for several enzymes and processes (3), although a signaling role has not been considered. PP_i can be generated by glycolysis, oxidative phosphorylation, and photophosphorylation and can replace ATP in a number of reactions (4). The cytosolic concentration of PP_i is regulated in eukaryotic cells by soluble PPases (5).

An unusual characteristic of *Trypanosoma brucei*, the etiologic agent of sleeping sickness or African trypanosomiasis, and of other trypanosomatids is that they possess higher cellular levels of PP_i than of ATP (6). Most PP_i, as well as polyphosphate (polyP), is stored in acidic organelles named acidocalcisomes (7). Acidocalcisomes from *T. brucei* are electron dense and possess large amounts of cations bound to polyP, with several pumps in their membranes, like the vacuolar proton pyrophophatase (V-H^+-PPase), which contributes to their acidification (8). When fixed *Trypanosoma cruzi* (9) or *Trypanosoma evansi* (10) cells are treated with PPase, the electron-dense matrix of

Citation Potapenko E, Cordeiro CD, Huang G, Docampo R. 2019. Pyrophosphate stimulates the phosphate-sodium symporter of *Trypanosoma brucei* acidocalcisomes and *Saccharomyces cerevisiae* vacuoles. mSphere 4:e00045-19. https://doi.org/10.1128/mSphere.00045-19.

Editor Margaret Phillips, University of Texas Southwestern

Address correspondence to Roberto Docampo, rdocampo@cb.uga.edu.

E.P. and C.D.C. contributed equally to this work.

Inorganic pyrophosphate as a signaling molecule

Received 25 January 2019
Accepted 14 March 2019
Published 3 April 2019

acidocalcisomes is removed, indicating that PP_i is a component of this organelle's structure. Besides the acidocalcisomal V-H^+-PPase, other enzymes of *T. brucei*, such as a soluble pyrophosphatase (11–13), and the glycosomal pyruvate-phosphate dikinase (14) can use PP_i.

Recent work has shown that a phosphate-sodium symporter from both *T. brucei* acidocalcisomes (TbPho91) and *Saccharomyces cerevisiae* vacuoles (Pho91p) is stimulated to release P_i and Na^+ to the cytosol by the binding of inositol hexakisphosphate (IP_6) or diphosphoinositol pentakisphosphate (5-PP-IP_5 or 5-IP_7) to their SPX domain (15). PP_i is formed by biosynthetic reactions, like the synthesis of deoxynucleotide triphosphates (dNTPs) that are needed for yeast DNA duplication (16) or for the biosynthesis of phospholipids and nucleotides needed for cell duplication (17). These reactions require an abundant source of P_i. We therefore considered a potential signaling role of PP_i in the export of vacuolar P_i. Heterologously expressed *TbPHO91*, with or without its SPX domain, in *Xenopus* oocytes was tested by the two-electrode voltage clamp method to measure transmembrane currents in the presence of PP_i and polyphosphates. We also prepared giant vacuoles of yeast expressing either wild-type or *T. brucei* Na^+/P_i symporters and patch-clamped them. We report that PP_i stimulates TbPho91 and Pho91p, leading to P_i and Na^+ release to the cytosolic side of the vacuoles, and that the presence of an SPX domain in TbPho91 is important for this stimulation to occur.

RESULTS

Modulation of the Na^+/P_i conductance of TbPho91 by pyrophosphate and polyphosphates. TbPho91 localizes to acidocalcisomes (18), and these organelles are rich in PP_i (6). Therefore, we examined whether this compound induced net inward currents when applied to *Xenopus* oocytes expressing the symporter. Figure 1A shows the inward current generated at holding potential ($V_h = -60$ mV) by the addition of equimolar concentrations of P_i or PP_i. The current amplitude induced by PP_i was a few hundred nanoamperes and was larger than that induced by P_i (Fig. 1A and B). One possible reason for the induction of these inward currents is the cotransport of Na^+ and PP_i, through TbPho91. However, while there is Na^+-dependent uptake of $^{32}P_i$, there is no significant Na^+-dependent $^{32}PP_i$ uptake into oocytes expressing TbPho91 (Fig. 1C). The results suggest that while PP_i is not transported, Na^+ transport, which generates an inward current, is stimulated by PP_i. Interestingly, when PP_i was added before P_i, P_i induced larger current amplitudes than when added alone, indicating that PP_i has a modulating effect on Na^+ transport through TbPho91 (Fig. 1D).

PolyPs of different lengths induce inward currents in a pH- and calcium-dependent manner in oocytes expressing *TbPho91 and PHO91*. When polyPs of different lengths were used, similar inductions of inward currents were observed. $PolyP_3$ (tripolyphosphate or TPP) induced currents of larger amplitude than $polyP_{100}$ or $polyP_{700}$ (Fig. 2A), and similar results were observed when *S. cerevisiae* Na^+/P_i cotransporter (*PHO91*) was expressed in oocytes (Fig. 2B). However, when we used the same concentration of PP_i and $polyP_3$ in phosphate units as with the longer polyPs, the amplitude changes were not significantly different (data not shown). Peak amplitudes of inward currents in oocytes expressing *TbPho91* (in nanoamperes) were as follows: 250.1 ± 40.4 ($n = 4$) for PP_i, 416.3 ± 47.4 ($n = 4$) for $polyP_3$, 119 ± 69.6 ($n = 5$) for $polyP_{100}$, and 333.5 ± 45.6 ($n = 4$) for $polyP_{700}$ (Fig. 2A, right panel). In oocytes expressing yeast *PHO91*, the amplitudes of inward currents (in nanoamperes) were as follows: 447.8 ± 84.1 ($n = 5$) for PP_i, 771.6 ± 168.4 ($n = 5$) for $polyP_3$, 312.4 ± 50.8 ($n = 5$) for $polyP_{100}$, and 142.8 ± 23.5 ($n = 5$) for $polyP_{700}$ (Fig. 2B, right panel). The control amplitudes of Na^+/P_i currents in *TbPho91*- and *PHO91*-expressing oocytes were 157.1 ± 32.8 nA and 146.8 ± 41.6 nA ($n = 4$), respectively (Fig. 2A and B, right panels).

Similar to P_i-induced currents (15), polyP-induced currents also depended on extracellular pH (Fig. 2C). Acidification of the extracellular medium inhibited TbPho91 currents induced by the application of 10 mM $polyP_3$. The amplitude of the Na^+/polyP transient was significantly lower at pH 6.8 (203.5 ± 12 nA, $P < 0.0001$, $n = 8$) and pH 6.2

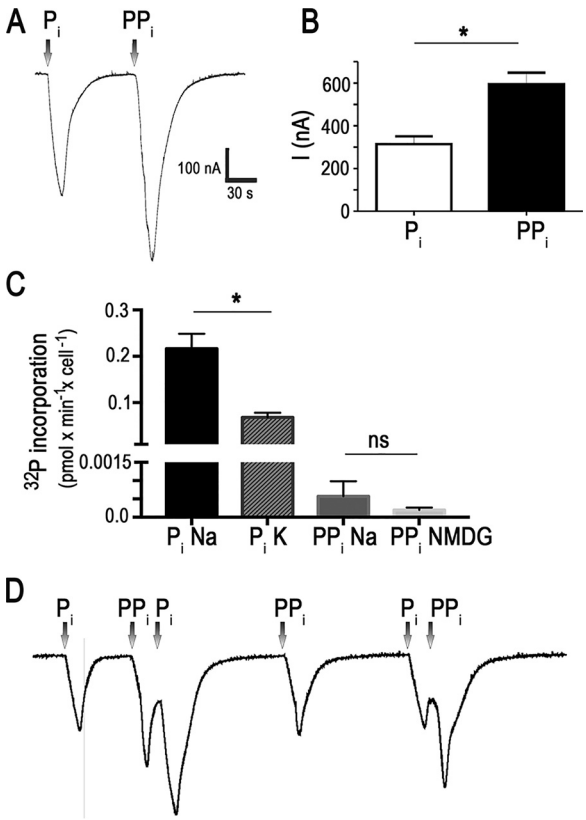

FIG 1 Effect of PP_i on P_i-elicited currents in oocytes expressing TbPho91 and P_i and PP_i uptake by the same oocytes. (A) Representative currents recorded after the addition of 10 mM Na^+/P_i or 10 mM Na^+/PP_i to oocytes expressing TbPho91. (B) Quantification of results from several experiments as described for panel A. (C) ^{32}P incorporation of $Na^+/^{32}P_i$, $K^+/^{32}P_i$, $Na^+/^{32}PP_i$, or NMDG/$^{32}PP_i$ into oocytes expressing TbPho91. (D) Representative currents after sequential addition of 10 mM Na^+/P_i or 10 mM Na^+/PP_i to oocytes expressing TbPho91. Values in panels B and C are means ± SEM; $n = 6$ (B) and $n = 3$ (C). *, $P < 0.05$ (Student's *t* test); ns, not significant.

(56 ± 5.7 nA, $P < 0.0001$, $n = 8$) than at pH 7.0 (424.1 ± 65 nA). This effect was reversible in the course of tens of minutes in medium at neutral pH. However, a shift to more alkaline pH values (up to pH 7.8) did not produce significant changes in current (Fig. 2D). Figure 2E shows means ± standard errors of the means (SEM) of the results of three experiments.

Decreasing the extracellular calcium concentration ($[Ca^{2+}]_{out}$) from 1.8 mM to 100 and 10 μM induced an increase in $polyP_3$ current from 426.4 ± 36.6 nA to 564.8 ± 41 nA ($P < 0.05$, $n = 8$) and 534.8 ± 69.6 nA ($P < 0.05$, $n = 4$), respectively (Fig. 2F and G). In addition, the kinetics of the $polyP_3$ current transient was also changed, showing a slow decay in restoration to the basal level, especially at 10 μM $[Ca^{2+}]_{out}$ (Fig. 2F). Thus, the half-width of the current transient increased (in seconds) from 23.9 ± 2.3 at 1.8 $[Ca^{2+}]_{out}$ to 46.8 ± 6.4 ($P < 0.05$, $n = 4$) and 73.7 ± 10.8 ($P < 0.01$, $n = 4$) at 100 μM and 10 μM $[Ca^{2+}]_{out}$, respectively (Fig. 2H). An increase of $[Ca^{2+}]_{out}$ above 3.0 mM led to oocyte death within minutes.

Taken together, the results suggest that PP_i and polyPs might be modulating the opening of the Na^+/P_i cotransporter and facilitating Na^+ transport and generation of the currents in a pH- and calcium-dependent manner.

Modulation of the Na^+/P_i conductance of TbPho91 by pyrophosphate is dependent on the SPX domain. It has been recognized that the SPX domains present in the N termini of vacuolar transporter chaperones, signaling proteins, and phosphate transporters can function as polyphosphate sensor domains (19). They bind to phosphate-containing ligands like PP_i, $polyP_3$, and IP_6 at micromolar levels and to 5-IP_7

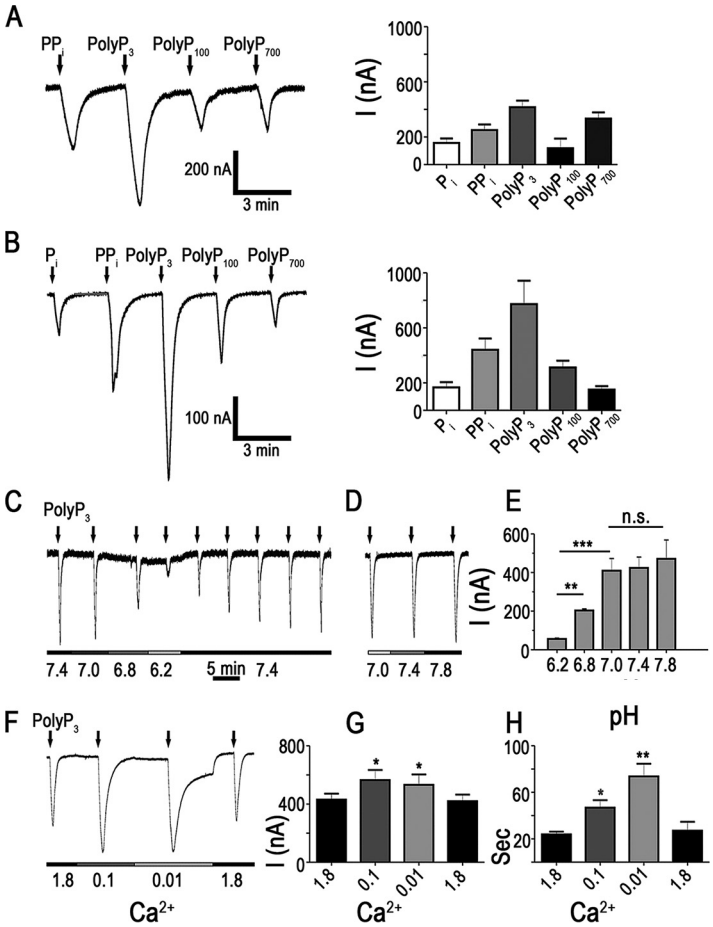

FIG 2 Currents elicited by PP_i and polyPs in oocytes expressing TbPho91 and Pho91p. (A) Representative currents recorded after the addition of 10 mM Na^+/PP_i, $Na^+/polyP_3$, $Na^+/polyP_{100}$, and $Na^+/polyP_{700}$ to oocytes expressing TbPho91. The right panel shows the quantification of currents elicited from four experiments. (B) Representative currents recorded after the addition of 10 mM Na^+/PP_i, $Na^+/polyP_3$, $Na^+/polyP_{100}$, and $Na^+/polyP_{700}$ to oocytes expressing Pho91p. The right panel shows the quantification of currents elicited from four experiments. (C to E) Currents recorded in response to the addition of 10 mM $Na^+/polyP_3$ at different pH levels (C and D) and quantification of the results of three experiments (E). (F to H) Currents recorded in response to the addition of 10 mM $Na^+/polyP_3$ at different Ca^{2+} concentrations (F) and quantification of the current intensity (G) or current duration (H) of several experiments. Values in panels E, G, and H are means ± SEM; $n = 4$. *, $P < 0.05$; **, $P < 0.01$; ***, $P < 0.001$; n.s., not significant (Student's *t* test). Concentrations of $Na^+/polyP_{100}$ and $Na^+/polyP_{700}$ are expressed in phosphate units.

at nanomolar concentrations. Similarly, we found that IP_6 and 5-IP_7 stimulate the yeast and *T. brucei* Na^+/P_i symporter through its SPX domain (15). We therefore investigated whether this was also the case with PP_i.

In addition to the ability of PP_i to directly activate TbPho91, it can also modulate the Na^+/P_i current. When oocytes were preincubated for 5 to 6 min with PP_i, in the micromolar range (Fig. 3A), there was an induction of slow inward currents, followed by amplification of the Na^+/P_i-transmembrane current evoked by 10 mM P_i. The thresholds for statistically significant amplification of the Na^+/P_i current were 100 μM for PP_i (13.5% ± 0.87% higher than the reference value, $P < 0.05$, $n = 5$) (Fig. 3B) and 200 μM for $polyP_3$ (+15.7%, $P < 0.05$, $n = 4$) (Fig. 3C and D).

To examine the role of the SPX domain of TbPho91 in this stimulation by PP_i, we expressed the protein with a deletion of this domain (TbPho91-ΔSPX) (15) and measured its response to PP_i. When *TbPho91-ΔSPX*-expressing oocytes were tested, no amplification of the currents induced by 10 mM P_i occurred by the addition of PP_i (Fig. 3B), which confirms previous findings on the role of the SPX domain in regulating Phop91p conductance.

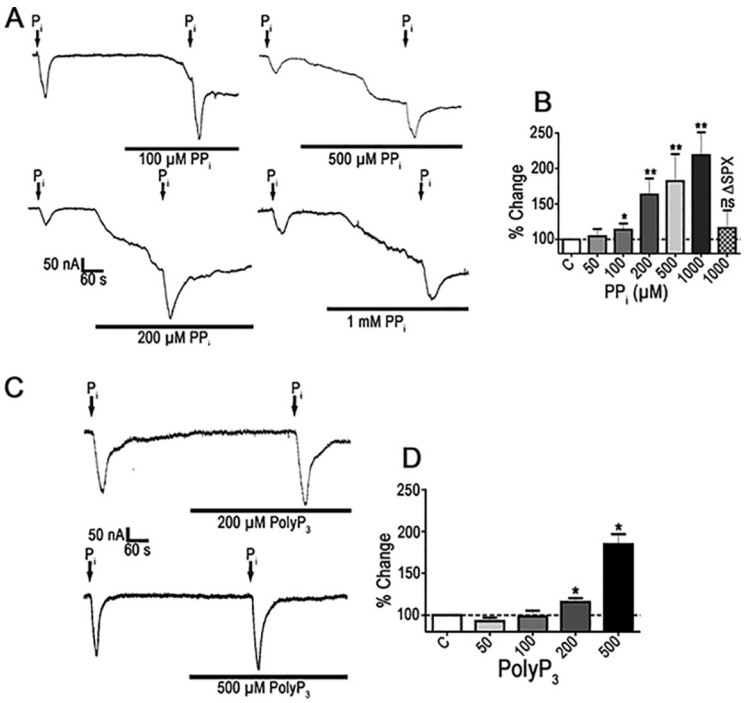

FIG 3 Effect of PP_i on P_i-elicited currents in oocytes expressing TbPho91. (A) Representative currents recorded when the addition of 10 mM Na^+/P_i was done in the absence or presence of the indicated concentrations of PP_i. (B) Quantification of the results of several experiments as described for panel A. C, control. (C) Representative currents recorded when the addition of 10 mM Na^+/P_i was done in the absence or presence of the indicated concentrations of $polyP_3$. (D) Quantification of the results of several experiments as described for panel C. C, control. Values in panels B and D are means ± SEM; $n = 4$. *, $P < 0.05$; **, $P < 0.01$ (Student's *t* test).

Stimulation of Na^+/P_i release by PP_i from yeast vacuoles. We applied the spheroplast incubation method to prepare giant cells of *S. cerevisiae* by using 2-deoxyglucose to inhibit cell wall synthesis (20). The giant cells were treated by moderate hyposmotic shock to disrupt the plasma membrane and release the enlarged vacuoles. A patch pipette was then attached to the vacuolar membrane, and after formation of a gigaseal, the patch membrane was ruptured by high-voltage pulses. The lumen of the vacuole was connected to the pipette (whole-vacuole configuration) and was loaded with a solution containing Na^+ and P_i, to record transmembrane currents. We used *pho91*Δ cells to express *TbPHO91*.

Patch-clamp recordings of the vacuoles were performed at a V_h of +60 mV. The bath solution had 10 mM HEPES, pH 7.1, containing 100 mM NaCl, 200 mM sorbitol, and 1 mM $MgCl_2$, while the pipette solution contained a similar solution plus 10 mM NaH_2PO_4-Na_2HPO_4 in order to detect outward currents generated by displacement of Na^+/P_i to the bath solution ("cytosol"). After 10 mM PP_i was added to the bath solution (Fig. 4A), we registered outward currents of 60.3 ± 12.7 pA ($n = 3$) in vacuoles from wild-type cells. When vacuoles from *pho91*Δ cells were used, no significant currents were detected after PP_i application (Fig. 4B).

We then expressed *TbPHO91* in giant vacuoles of *pho91*Δ cells. Application of 10 mM PP_i induced outward currents of 22.3 ± 3.7 pA ($n = 3$) (Fig. 4C and D). Our results demonstrate that PP_i triggers the release of Na^+/P_i by the Pho91 symporters.

DISCUSSION

We report here that functional expression in *Xenopus laevis* oocytes of *T. brucei* or *S. cerevisiae* Na^+/P_i symporter Pho91, followed by two-electrode voltage clamp recordings, showed that the application of PP_i or polyP resulted in the depolarization of the oocyte membrane potential and an increase in the P_i conductance. The stimulation

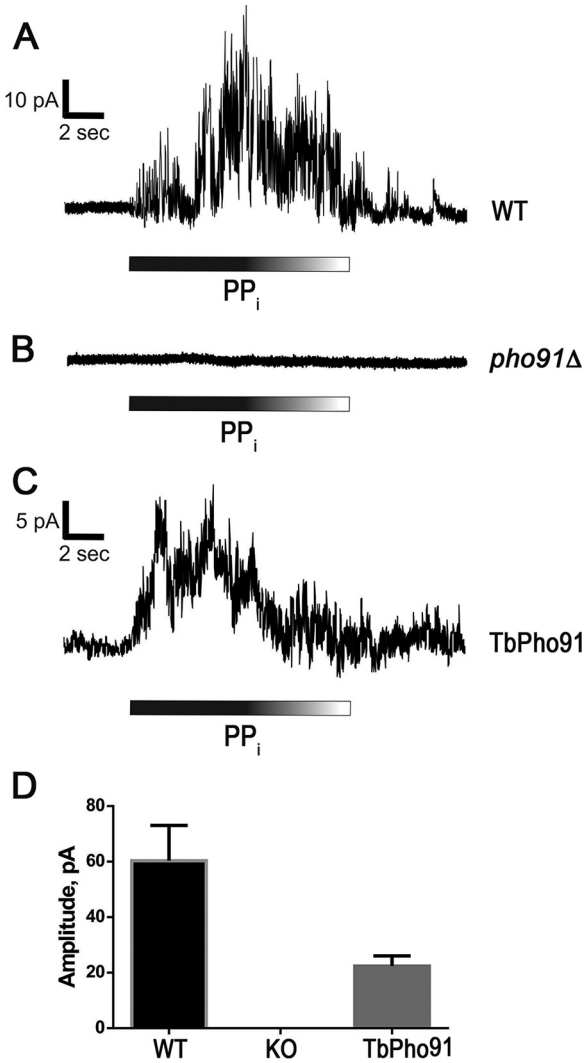

FIG 4 PP_i induces activation of Na^+/Pi currents in Pho91- and TbPho91-expressing yeast vacuoles. (A) Activation of Na^+/Pi outward currents in vacuoles from wild-type yeast after the addition of 10 mM PP_i. (B) *pho91*Δ vacuoles do not produce currents after application of PP_i. (C) Complementation of *pho91*Δ with *TbPHO91* restores vacuole response to PP_i. Data are representative of two to four independent experiments and are quantified in panel D. We used at least four successful current recordings for each experiment. About 80% of the vacuoles showed clear responses. WT, wild type; KO, knockout.

induced by PP_i was abolished when the SPX domain of the symporter was deleted. Application of PP_i to yeast giant vacuoles expressing TbPho91 or Pho91p but not to vacuoles of *pho91*Δ cells induced outward currents, suggesting a role of PP_i in Na^+/P_i release.

Pyrophosphate does not penetrate *Xenopus* oocytes, but it stimulates the Pho91 transporters that are expressed in them. If this happens through the SPX domain, the domain would have to be oriented toward the exterior of the oocyte. Plasma membrane orientation is essentially demonstrated by positive functionality. The best evidence that the topology of Pho91 and TbPho91 in *Xenopus* oocytes is inverted is that Na^+ and P_i are transported into the oocytes, as demonstrated by electrophysiological recordings and $^{32}P_i$ uptake experiments. This does not occur in the giant vacuoles, where we detected P_i release to the cytosolic side of the vacuole. The currents detected are due to the electrogenic nature of the transporter (Na^+ is the charge carrier, and P_i without Na^+ does not elicit currents [15]). The transfer of Na^+ to the cytosol is favored by the higher Na^+ concentration in the extracellular medium. In contrast, acidocalcisomes and yeast vacuoles have more Na^+ than the cytosol and Na^+ efflux is favored.

This inversion of the membrane topology in the plasma membrane of *Xenopus* oocytes indicates that the amino-terminal region containing the SPX domain is also inverted and oriented toward the outside, as demonstrated by the experiments with expression of truncated TbPho91. This is also in agreement with structural data available for other P_i transporters (21) that showed that there is no reorientation of the carrier alternatively exposing the substrate binding sites to one or the other side of the membrane, as previously postulated (22, 23), but movement of ions within the transmembrane field. It is known that lipid composition can affect topology of a membrane protein, or orientation of its α-helices in a membrane, which underlies membrane protein function. Inversion of the membrane topology of vacuolar transporters expressed in the plasma membrane of *Xenopus* oocytes is not infrequent (24).

Our results concerning the role of the SPX domain in the yeast Pho91p is at variance with its role in the plasma membrane low-affinity P_i transporters Pho87p and Pho90p (25). When the SPX domain was removed to generate a truncated form of Pho90p, there was increased accumulation of phosphate, which was proposed as evidence that SPX is a regulatory domain that inhibits phosphate transport under normal conditions (25). However, the SPX removal experiments did not provide mechanistic evidence on how SPX regulates the transporters. Electrophysiological characterization of Pho90p and Pho87p could reveal whether polyphosphate-containing molecules (or the Slp2 protein), acting on the SPX domain, regulate phosphate uptake by these low-affinity transporters.

It was shown before that 1 mM PP_i "primes" (26) or stimulates the catalytic domain of the polyP polymerase vacuolar transporter chaperone 4 (VTC4) of *S. cerevisiae* but inhibits the catalytic domain of *T. brucei* VTC4 (27). PP_i and $polyP_3$ also bind to the SPX domain of *S. cerevisiae* VTC2, as determined by isothermal titration calorimetry, with dissociation constants (K_d) of 154 $\pm$ 62 and 11.1 $\pm$ 1.7 μM, respectively, but PP_i does not significantly stimulate VTC-catalyzed polyP synthesis by isolated yeast vacuoles at millimolar concentrations (26). We found that the threshold for PP_i for statistically significant amplification of the Na^+/P_i current in *Xenopus* oocytes expressing *TbPho91* was 100 μM, which is within the physiological levels of cytosolic PP_i in several cell types. For example, the PP_i concentration in the cytosol of plant cells is about 0.2 to 0.3 mM (28), while in exponentially growing *Escherichia coli* K-12 cells, the intracellular PP_i concentration is about 0.5 mM, even after varying the amount of pyrophosphatase from 15 to 2,600% of the control amount (29). In addition, the PP_i content in *E. coli* can be increased up to 2.5 mM when the growth of cells is limited by inhibition of the synthesis of nucleotides (30). The concentration of PP_i in different species has been reviewed extensively, and, for example, it has been estimated to be at about 100 to 200 μM in rat liver (3).

Although $polyP_3$ and other polyPs are able to induce inward currents in *Xenopus* oocytes expressing *TbPho91*, their physiological relevance is relative, as most of these compounds are compartmentalized in the acidocalcisomes (6, 7), nucleolus, and glycosomes (31). In this regard, it has been demonstrated the polyP is toxic when in the yeast cytosol (32). We do not think that polyPs could have a physiological role, and we attribute their stimulatory effect to their chemical similarities to PP_i.

In conclusion, our work revealed that PP_i stimulates the Na^+/P_i symporter of *T. brucei* acidocalcisomes, and that of its yeast ortholog localized in the vacuole, through its SPX domain. This stimulation results in the release of P_i and Na^+ to the cytosolic side of the vacuoles. Our hypothesis is that as result of enhanced PP_i production by anabolic reactions, the increase in PP_i would stimulate the P_i release needed for these anabolic reactions (Fig. 5). The results reveal an unrecognized role of PP_i in cell signaling.

MATERIALS AND METHODS

Chemicals and reagents. Integrated DNA Technologies (Coralville, IA) provided the primers used. All other reagents of analytical grade were purchased from Sigma-Aldrich (St. Louis, MO).

Cell cultures. *T. brucei* (Lister 427 strain procyclic forms [PCF]) were grown at 28°C in SDM-79 medium (33) with 10% heat-inactivated fetal bovine serum and hemin (7.5 μg/ml).

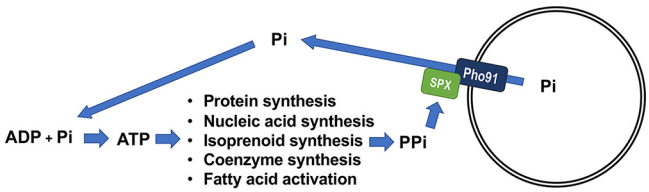

FIG 5 Schematic representation of PP_i signaling function. Large amounts of P_i are needed for biosynthetic pathways, which generate PP_i as a by-product. PP_i stimulates the vacuolar Pho91 Na^+/P_i symporters through their SPX domains, increasing the release of P_i needed for ATP biosynthesis.

Yeast strains. We used *S. cerevisiae* strain BY4741 (*MATa his3Δ1 leu2Δ0 met15Δ0 ura3Δ0*). Generation of *pho91*Δ was as described previously (15).

Preparation and isolation of giant yeast vacuoles. Preparation of giant yeast vacuoles from the wild type and *pho91*Δ mutants was done as described before (20), with minor modifications (15). The vacuoles were attached to a poly-L-lysine-coated chamber for patch-clamp recording. The micropipette solution contained 10 mM HEPES, pH 7.1, 100 mM NaCl, 200 mM sorbitol, 1 mM $MgCl_2$, 5 mM NaH_2PO_4, and 5 mM Na_2HPO_4. The bath solution was similar, but without NaH_2PO_4, and Na_2HPO_4.

Preparation and maintenance of oocytes. *Xenopus laevis* oocytes were obtained from Xenoocyte (Dexter, MI). Oocytes collected at stage IV or V were manually defolliculated and devitellinized with collagenase (1 mg/ml) for 1 h at room temperature and then maintained in filtered modified Barth's solution containing 88 mM NaCl, 1 mM KCl, 0.82 mM $MgSO_4$, 0.41 mM $CaCl_2$, 2.4 mM $NaHCO_3$, 0.33 mM $Ca(NO_3)_2$, and 10 mM HEPES, plus 50 μg/ml gentamicin, pH 7.4, at a density of less than 100 per 60-mm plastic petri dish. Barth's solution was replaced daily.

cRNA production, oocyte injection, and electrophysiology. PrimeSTAR HS DNA polymerase (Clontech) was used to amplify by PCR full-length *TbPHO91* (Tb427tmp.01.2950), truncated *TbPHO91* (*TbPHO91-ΔSPX*; obtained by removal of the 606-nucleotide sequence encoding the N-terminal putative SPX domain), and *PHO91* (GenBank accession number NM_001183190) open reading frames (15) from *T. brucei* or *S. cerevisiae* genomic DNA, using the corresponding gene-specific primers indicated in Table 1. The PCR products were purified as described previously (15), and the nucleotide sequences were confirmed by sequencing. cRNAs were obtained by *in vitro* transcription using the purified PCR products as the templates with an mMESSAGE mMACHINE kit (Ambion Life Technologies, Thermo Fisher Scientific, Inc, Waltham, MA), in accordance with the manufacturer's protocol, and verified as described previously (15). cRNA injection was done exactly as described before (15). Equal amounts of cRNA from control and mutant transporters were injected into the *Xenopus* oocytes. For electrophysiology, the standard two-electrode voltage-clamp technique was used, as described previously (15). At least four oocytes from two different frogs were used in each experiment. All recordings were obtained at room temperature. Oocytes were bathed in ND96 buffer bath solution containing 96 mM NaCl, 2 mM KCl, 5 mM $MgSO_4$, 1 mM $CaCl_2$, and 2.5 mM HEPES, pH 7.5, with a continuous perfusion speed of ~2 ml/min. Low-calcium solutions were prepared by adding Ca^{2+} and EGTA at proportions calculated with MaxChelator software (Stanford University, CA). The required pH of ND96 was adjusted either with NaOH or HCl. The effect of PP_i and polyphosphates was studied by their addition to ND96 with subsequent pH readjustments. To

TABLE 1 Primers used in this study

Primer sequence[a]	Use[b]
AGGAAAAATGCCGCTCAAAATCT	Knockout of yeast *PHO91*
CAATACAAATGGGCATTGACCAGA	Knockout of yeast *PHO91*
TTGGGTACCGGGCCCCCCCTCGAGGTGGGCCTATCCGCCTTAAT	Amplification of *PHO91* for cloning in pRS413
GGATCCCCCGGGCTGCAGGAATTCAATCATAAGTGGTGCGGCCA	Amplification of *PHO91* for cloning in pRS413
GACACGGTAACTTGCAGACTGACATGAAGTTCGGAAAGCG	Amplification of *TbPHO91* for fusing with *PHO91* UTRs and cloning in pRS413
TTTCATTCTCTCTATGGATAATCCTACGGTTTGCCTTCAAA	Amplification of *TbPHO91* for fusing with *PHO91* UTRs and cloning in pRS413
TTGGGTACCGGGCCCCCCCTCGAGGTGGGCCTATCCGCCTTAAT	Amplification of *PHO91* 5′ UTR for fusing with *TbPHO91*
GTCAGTCTGCAAGTTACCGTGTCACCTTCACAGTTTTCTTTTTATTTG	Amplification of *PHO91* 5′ UTR for fusing with *TbPHO91*
GATTATCCATAGAGAGAATGAAAGGTTACTAATATAGTATGTATACGTGC	Amplification of *PHO91* 3′ UTR for fusing with *TbPHO91*
GGATCCCCCGGGCTGCAGGAATTCAATCATAAGTGGTGCGGCCA	Amplification of *PHO91* 3′ UTR for fusing with *TbPHO91*
CCCGCGAAATTAATACGACTCACTATAGGGAGA**CCACC***ATGAAGTTCGGAAAGCGGC*	*TbPHO91T7F* (for *Xenopus* expression)
CCCGCGAAATTAATACGACTCACTATAGGGAGA**CCACC***ATGGAAGCAGAGATTAGCCG*	*TbPHO91TFN* (for *Xenopus* expression)
TTTTTTTTTTTTTTTTTTTTTTTTTTTTTT*CTACGGTTTGCCTTCAAACAC*	*TbPHO91T30R* (for *Xenopus* expression)
CCCGCGAAATTAATACGACTCACTATAGGGAGA**CCACC***ATGAAGTTCTCGCATTCCT*	*PHO91T7F* (for *Xenopus* expression)
TTTTTTTTTTTTTTTTTTTTTTTTTTTTTT*CTAAAATCCCATTACTTTCAATATGCC*	*PHO91T30R* (for *Xenopus* expression)

[a]For the last five primers, T_7 promoter or polyT_{30} sequences are underlined. Kozak consensus sequences for increasing efficiency of translation initiation are in bold. Gene-specific sequences are italicized. Additional nucleotides upstream of the T_7 promoter or the Kozak consensus sequence are incorporated into the primers for desirable *in vitro* transcription/translation in *Xenopus laevis* oocytes.

[b]UTR, untanslated region.

prepare the phosphate solution, 300 mM stock solutions of mono- and dibasic sodium phosphates were mixed until pH 7.4 was obtained.

Yeast giant vacuole experiments were done exactly as described previously (15). All recordings were performed at a V_h of +60 mV. An Axopatch 200b amplifier was used for current registration, and data were filtered at 1,000 Hz, digitized with Digidata 1550A (Axon Instruments, USA), and analyzed offline using PClamp 10 software.

^{32}P and ^{32}PP uptake assays. *Xenopus laevis* oocytes were injected with cRNA as described above and used after 3 days. Oocytes were incubated in standard ND96 solution or a modified ND96 solution with sodium replaced by an equimolar concentration of potassium or NMDG (ND96–Na). The healthiest looking oocytes were transferred to Eppendorf tubes (6 per tube) and incubated with 200 μl of ND96 or ND96–Na solutions containing 300,000 cpm of inorganic ^{32}P (60 Ci/mmol) or ^{32}P-labeled pyrophosphate (60 Ci/mmol) (Perkin Elmer). Oocytes were then incubated for 30 min at room temperature and washed five times with 1 ml of ND96 or ND96–Na. Prolonged incubation of oocytes under these conditions decreased the oocyte quality, probably due to strong and long-lasting depolarization of the cellular membrane. Oocytes were then lysed with 10% sodium dodecyl sulfate (SDS), and the total lysate was added to the scintillation cocktail (MP Biomedicals). ^{32}P radiation was measured using an LS 6500 multipurpose scintillation counter (Beckman Coulter). Each of three experiments was done using triplicate measurements.

Statistical analysis. All values are expressed as means ± SEM, unless indicated otherwise. Significant differences between treatments were compared using unpaired Student's *t* tests. Differences were considered statistically significant at a P of <0.05, and n refers to the number of independent biological experiments performed. All statistical analyses were conducted using GraphPad Prism 6 (GraphPad Software, San Diego, CA).

ACKNOWLEDGMENTS

We thank Vincent J. Starai for advice on the preparation of yeast mutants.

This work was funded by a grant from the U.S. National Institutes of Health (AI-077358 to R.D.). E.P. was supported by a training grant (T32 AI060546) from the U.S. National Institutes of Health.

REFERENCES

1. Orriss IR, Arnett TR, Russell RG. 2016. Pyrophosphate: a key inhibitor of mineralisation. Curr Opin Pharmacol 28:57–68. https://doi.org/10.1016/j.coph.2016.03.003.
2. Kornberg A. 1957. Pyrophosphorylases and phosphorylases in biosynthetic reactions. Adv Enzymol Relat Subj Biochem 18:191–240.
3. Heinonen JK. 2001. Biological role of inorganic pyrophosphate. Springer, New York, NY.
4. Lahti R. 1983. Microbial inorganic pyrophosphatases. Microbiol Rev 47:169–178.
5. Veech RL, Cook GA, King MT. 1980. Relationship of free cytoplasmic pyrophosphate to liver glucose content and total pyrophosphate to cytoplasmic phosphorylation potential. FEBS Lett 117(Suppl):K65–K72. https://doi.org/10.1016/0014-5793(80)80571-0.
6. Moreno B, Urbina JA, Oldfield E, Bailey BN, Rodrigues CO, Docampo R. 2000. 31P NMR spectroscopy of *Trypanosoma brucei, Trypanosoma cruzi,* and *Leishmania major*. Evidence for high levels of condensed inorganic phosphates. J Biol Chem 275:28356–28362. https://doi.org/10.1074/jbc.M003893200.
7. Docampo R, de Souza W, Miranda K, Rohloff P, Moreno SN. 2005. Acidocalcisomes–conserved from bacteria to man. Nat Rev Microbiol 3:251–261. https://doi.org/10.1038/nrmicro1097.
8. Rodrigues CO, Scott DA, Docampo R. 1999. Characterization of a vacuolar pyrophosphatase in *Trypanosoma brucei* and its localization to acidocalcisomes. Mol Cell Biol 19:7712–7723. https://doi.org/10.1128/MCB.19.11.7712.
9. Urbina JA, Moreno B, Vierkotter S, Oldfield E, Payares G, Sanoja C, Bailey BN, Yan W, Scott DA, Moreno SN, Docampo R. 1999. *Trypanosoma cruzi* contains major pyrophosphate stores, and its growth in vitro and in vivo is blocked by pyrophosphate analogs. J Biol Chem 274:33609–33615. https://doi.org/10.1074/jbc.274.47.33609.
10. Mendoza M, Mijares A, Rojas H, Rodriguez JP, Urbina JA, DiPolo R. 2002. Physiological and morphological evidences for the presence acidocalcisomes in *Trypanosoma evansi*: single cell fluorescence and ^{31}P NMR studies. Mol Biochem Parasitol 125:23–33. https://doi.org/10.1016/S0166-6851(02)00166-4.
11. Lemercier G, Espiau B, Ruiz FA, Vieira M, Luo S, Baltz T, Docampo R, Bakalara N. 2004. A pyrophosphatase regulating polyphosphate metabolism in acidocalcisomes is essential for *Trypanosoma brucei* virulence in mice. J Biol Chem 279:3420–3425. https://doi.org/10.1074/jbc.M309974200.
12. Kotsikorou E, Song Y, Chan JM, Faelens S, Tovian Z, Broderick E, Bakalara N, Docampo R, Oldfield E. 2005. Bisphosphonate inhibition of the exopolyphosphatase activity of the *Trypanosoma brucei* soluble vacuolar pyrophosphatase. J Med Chem 48:6128–6139. https://doi.org/10.1021/jm058220g.
13. Yang Y, Ko T-P, Chen C-C, Huang G, Zheng Y, Liu W, Wang I, Ho M-R, Hsu S-TD, O'Dowd B, Huff HC, Huang C-H, Docampo R, Oldfield E, Guo R-T. 2016. Structures of trypanosome vacuolar soluble pyrophosphatases: antiparasitic drug targets. ACS Chem Biol 11:1362–1371. https://doi.org/10.1021/acschembio.5b00724.
14. Bringaud F, Baltz D, Baltz T. 1998. Functional and molecular characterization of a glycosomal PP_i-dependent enzyme in trypanosomatids: pyruvate, phosphate dikinase. Proc Natl Acad Sci U S A 95:7963–7968. https://doi.org/10.1073/pnas.95.14.7963.
15. Potapenko E, Cordeiro CD, Huang G, Storey M, Wittwer C, Dutta AK, Jessen HJ, Starai VJ, Docampo R. 2018. 5-Diphosphoinositol pentakisphosphate (5-IP_7) regulates phosphate release from acidocalcisomes and yeast vacuoles. J Biol Chem 293:19101–19112. https://doi.org/10.1074/jbc.RA118.005884.
16. Bru S, Martínez-Laínez JM, Hernández-Ortega S, Quandt E, Torres-Torronteras J, Martí R, Canadell D, Ariño J, Sharma S, Jiménez J, Clotet J. 2016. Polyphosphate is involved in cell cycle progression and genomic stability in *Saccharomyces cerevisiae*. Mol Microbiol 101:367–380. https://doi.org/10.1111/mmi.13396.
17. Neef DW, Kladde MP. 2003. Polyphosphate loss promotes SNF/SWI- and Gcn5-dependent mitotic induction of PHO5. Mol Cell Biol 23:3788–3797. https://doi.org/10.1128/MCB.23.11.3788-3797.2003.
18. Huang G, Ulrich PN, Storey M, Johnson D, Tischer J, Tovar JA, Moreno SN, Orlando R, Docampo R. 2014. Proteomic analysis of the acidocalcisome, an organelle conserved from bacteria to human cells. PLoS Pathog 10:e1004555. https://doi.org/10.1371/journal.ppat.1004555.
19. Wild R, Gerasimaite R, Jung JY, Truffault V, Pavlovic I, Schmidt A, Saiardi A, Jessen HJ, Poirier Y, Hothorn M, Mayer A. 2016. Control of eukaryotic phosphate homeostasis by inositol polyphosphate sensor domains. Science 352:986–990. https://doi.org/10.1126/science.aad9858.
20. Yabe I, Horiuchi K, Nakahara K, Hiyama T, Yamanaka T, Wang PC, Toda K,

Hirata A, Ohsumi Y, Hirata R, Anraku Y, Kusaka I. 1999. Patch clamp studies on V-type ATPase of vacuolar membrane of haploid *Saccharomyces cerevisiae*. Preparation and utilization of a giant cell containing a giant vacuole. J Biol Chem 274:34903–34910. https://doi.org/10.1074/jbc.274.49.34903.

21. Pedersen BP, Kumar H, Waight AB, Risenmay AJ, Roe-Zurz Z, Chau BH, Schlessinger A, Bonomi M, Harries W, Sali A, Johri AK, Stroud RM. 2013. Crystal structure of a eukaryotic phosphate transporter. Nature 496: 533–536. https://doi.org/10.1038/nature12042.
22. Virkki LV, Biber J, Murer H, Forster IC. 2007. Phosphate transporters: a tale of two solute carrier families. Am J Physiol Renal Physiol 293: F643–F654. https://doi.org/10.1152/ajprenal.00228.2007.
23. Saliba KJ, Martin RE, Broer A, Henry RI, McCarthy CS, Downie MJ, Allen RJ, Mullin KA, McFadden GI, Broer S, Kirk K. 2006. Sodium-dependent uptake of inorganic phosphate by the intracellular malaria parasite. Nature 443:582–585. https://doi.org/10.1038/nature05149.
24. Wang C, Yue W, Ying Y, Wang S, Secco D, Liu Y, Whelan J, Tyerman SD, Shou H. 2015. Rice SPX-major facility superfamily 3, a vacuolar phosphate efflux transporter, is involved in maintaining phosphate homeostasis in rice. Plant Physiol 169:2822–2831. https://doi.org/10.1104/pp.15.01005..
25. Hurlimann HC, Pinson B, Stadler-Waibel M, Zeeman SC, Freimoser FM. 2009. The SPX domain of the yeast low-affinity phosphate transporter Pho90 regulates transport activity. EMBO Rep 10:1003–1008. https://doi.org/10.1038/embor.2009.105.
26. Hothorn M, Neumann H, Lenherr ED, Wehner M, Rybin V, Hassa PO, Uttenweiler A, Reinhardt M, Schmidt A, Seiler J, Ladurner AG, Herrmann C, Scheffzek K, Mayer A. 2009. Catalytic core of a membrane-associated eukaryotic polyphosphate polymerase. Science 324:513–516. https://doi.org/10.1126/science.1168120.
27. Lander N, Ulrich PN, Docampo R. 2013. *Trypanosoma brucei* vacuolar transporter chaperone 4 (TbVtc4) is an acidocalcisome polyphosphate kinase required for in vivo infection. J Biol Chem 288:34205–34216. https://doi.org/10.1074/jbc.M113.518993.
28. Weiner H. 1987. Subcellular localization of acetaldehyde oxidation in liver. Ann N Y Acad Sci 492:25–34. https://doi.org/10.1111/j.1749-6632.1987.tb48650.x.
29. Kukko-Kalske E, Lintunen M, Inen MK, Lahti R, Heinonen J. 1989. Intracellular PP_i concentration is not directly dependent on amount of inorganic pyrophosphatase in *Escherichia coli* K-12 cells. J Bacteriol 171: 4498–4500. https://doi.org/10.1128/jb.171.8.4498-4500.1989.
30. Kukko E, Saarento H. 1983. Accumulation of pyrophosphate in *Escherichia coli*. Relationship to growth and nucleotide synthesis. Arch Microbiol 136:209–211. https://doi.org/10.1007/BF00409846.
31. Negreiros RS, Lander N, Huang G, Cordeiro CD, Smith SA, Morrissey JH, Docampo R. 2018. Inorganic polyphosphate interacts with nucleolar and glycosomal proteins in trypanosomatids. Mol Microbiol 110:973–994. https://doi.org/10.1111/mmi.14131.
32. Gerasimaitė R, Sharma S, Desfougères Y, Schmidt A, Mayer A. 2014. Coupled synthesis and translocation restrains polyphosphate to acidocalcisome-like vacuoles and prevents its toxicity. J Cell Sci 127: 5093–5104. https://doi.org/10.1242/jcs.159772.
33. Cunningham I, Honigberg BM. 1977. Infectivity reacquisition by *Trypanosoma brucei brucei* cultivated with tsetse salivary glands. Science 197: 1279–1282. https://doi.org/10.1126/science.897667.